

Article

Property and Microstructure of Waterborne Self-Setting Geopolymer Coating: Optimization Effect of SiO₂/Na₂O Molar Ratio

Song Mu ^{1,2}, Jianzhong Liu ^{1,2,*}, Jiaping Liu ^{1,2}, Yaocheng Wang ³, Liang Shi ^{1,2} and Qian Jiang ^{1,2}

¹ SOBUTE New Materials Co., Ltd., Nanjing 211103, China; musong@cnjsjk.cn (S.M.); liujiaping@cnjsjk.cn (J.L.); shiliang@cnjsjk.cn (L.S.); jiangqian@cnjsjk.cn (Q.J.)

² State Key Laboratory of High Performance Civil Engineering Materials, Nanjing 210008, China

³ Shenzhen Key Laboratory of Civil Engineering Durability, Shenzhen University, Shenzhen 518060, China; wangyc_szu@126.com

* Correspondence: ljz@cnjsjk.cn

Received: 12 February 2018; Accepted: 13 April 2018; Published: 17 April 2018



Abstract: As a kind of coating material, the inorganic coating of alkali-activated metakaolin geopolymer cured at high temperature has been studied a lot for special applications. To our best knowledge, however, not much attention has been given to investigate the influence of SiO₂/Na₂O molar ratio on property of the geopolymer coating. This paper is, thus, dedicated to investigate the role of SiO₂/Na₂O molar ratio on property and microstructure of metakaolin-based geopolymer coating at ambient temperature. The effects on setting behavior, adhesive strength, shrinkage deformation and permeability are discussed. Multiple experiments were used to reveal microstructure changes of the geopolymer coating with different ratios of SiO₂/Na₂O, including Mercury Intrusion Porosimetry (MIP), Scanning Electron Microscope (SEM) and Fourier Transform Infrared Spectroscopy (FTIR). The results indicated that the optimal ratio of SiO₂/Na₂O was 1.0 for good properties of adhesive strength, shrinkage and impermeability. In addition, it has been found that the setting time of geopolymer coating increased with SiO₂/Na₂O ratio which increased from 0.8 to 1.5. That agrees well with the other property and results of exothermal rate of alkali-activated metakaolin. As for the microstructural changes, the SiO₂/Na₂O ratio of 1.0 reduced pore size and porosity of the geopolymer coating and particularly increased volume percentage of pores with a size lower than 20 nm. Besides, FTIR results suggested that geopolymer prepared by the ratio of 1.0 was likely to produce more heterogeneous geopolymer due to a greater silicate structural reorganization.

Keywords: inorganic coating; geopolymer; alkali-activated metakaolin; SiO₂/Na₂O ratio; property; microstructure

1. Introduction

With the increasing concern on green and ecofriendly requirements of coating, inorganic coating has gained more and more attention from academy and industry. Normally, inorganic coating can be categorized based on the main membrane substances, for example, silicates, colloidal silica and phosphate, etc. Recently, some studies have reported that geopolymer prepared by alkali-activated technology could be used to produce coatings [1–7].

Geopolymer is often made from alkali-activated aluminosilicate materials with or without calcium compounds. Based on alkali-activated technology, geopolymer displays a lower consumption of energy than traditional silicate cement, and produces a lower emission of carbon dioxide. Therefore, geopolymer is widely recognized as a promising material in civil engineering. During the past decades, many investigations on synthesis and characterization of geopolymer have been reported [8–11].

For synthesis of metakaolin-based geopolymer, calcination temperature, curing temperature and alkali-activated solution are important aspects. Normally, the alkali-activated solution is composed of alkali metals of silicate and hydroxide, for example, sodium silicate and sodium hydroxide. Sodium hydroxide is added into solution of sodium silicate that alternates $\text{SiO}_2/\text{Na}_2\text{O}$ ratio in order to effectively activate metakaolin particles. On one hand, alkali solution dissolved silicate and aluminate ions from metakaolin particles to start the geopolymerization process. On the other hand, soluble silicate species from sodium silicate solution provide some reactants for geopolymer reaction.

During the geopolymerization process, the $\text{SiO}_2/\text{Na}_2\text{O}$ molar ratio of alkali solution is used to represent amounts of free silicate species in alkali solution. Based on the geopolymerization mechanism, the free silicate species should contribute to polycondensation reaction between silicate hydroxyls. Meanwhile, silica ions in an oxygen-silicon tetrahedron can be replaced with aluminium ions dissolved from metakaolin particles to form zeolite crystals or amorphous phases. Unbalanced charge of aluminosilicate geopolymer due to the replacement diminishes with absorption of alkali metal ions.

Although the $\text{SiO}_2/\text{Na}_2\text{O}$ molar ratio is a vital parameter, few studies have been devoted to the influence of $\text{SiO}_2/\text{Na}_2\text{O}$ molar ratio on the property of geopolymer coating. The geopolymer coatings required curing at a high temperature to achieve good property rather than considering the role of $\text{SiO}_2/\text{Na}_2\text{O}$ molar ratio [2,5]. As matter of fact, Park et al. [12] reported strength of alkali-activated fly ash/slag continuously increased until exposure at 400 °C due to the decreased porosity. Besides, carbonation also contributes to increased strength of alkali-activated fly ash after curing at 80° in that formation of a high amount of binding gel [13]. In that way, optimization of $\text{SiO}_2/\text{Na}_2\text{O}$ molar ratio is helpful to improve the property of metakaolin-based geopolymer coating at a room temperature since a high curing temperature is not necessary. Therefore, the present paper studied changes of physical properties and microstructure of metakaolin-based geopolymer coating prepared by different ratios of $\text{SiO}_2/\text{Na}_2\text{O}$ at ambient temperature.

2. Materials and Methods

2.1. Materials

Metakaolin and alkali solution were used to prepare geopolymer. Metakaolin was produced by Hunan Super Chemical Co., Ltd., Changsha, China, and the pink appearance was presented after calcination at 700 to 900 °C. The chemical composition and particle size distribution (PSD) are shown in Table 1 and Figure 1, respectively. Table 1 shows that total content of SiO_2 and Al_2O_3 accounts for about 94% in metakaolin. According to the PSD, particle size of 90% of metakaolin is below 5.43 μm , and the average particle size is 1.73 μm .

Table 1. Chemical composition of metakaolin (wt %).

SiO_2	Al_2O_3	Fe_2O_3	CaO	MgO	K_2O	Na_2O	SO_3	LOI
60.85	34.51	0.95	0.5	0.39	0.19	0.34	1.82	0.88

Alkali solution is prepared by sodium silicate and sodium hydroxide. Sodium silicate was industrial grade water glass purchased from Nan Jing Baiyang Chemicals Co., Ltd., Nanjing, China, with a ratio of $\text{SiO}_2/\text{Na}_2\text{O}$ from 2.6 to 2.9. Solid content of the sodium silicate solution is 46.23% with a specific gravity of 1.45. In this study, $\text{SiO}_2/\text{Na}_2\text{O}$ ratio of sodium silicate was adjusted to 2 by addition of sodium hydroxide solution. Solutions were stored for a minimum of 24 h prior to use to allow homogenization; 12.5 mol/L of sodium hydroxide solutions were prepared by dissolution of NaOH powder (chemical purity, Sinopharm Chemical Reagent Co., Ltd., Shanghai, China) in tap water, and sealed in container to reduce the contamination by carbonation.

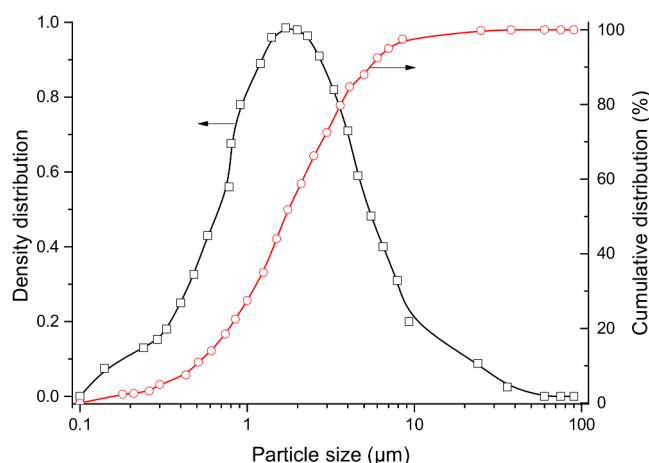


Figure 1. Particle size distribution of metakaolin.

Metakaolin-based geopolymers coating with different ratios of $\text{SiO}_2/\text{Na}_2\text{O}$ were prepared, as listed in Table 2. Metakaolin was dispersed by a mixer at a slow rate. Then alkali solution was added into the mixer and stirred moderately, until a homogeneous paste was attained.

Table 2. Mixtures of geopolymer coating with different ratios of $\text{SiO}_2/\text{Na}_2\text{O}$.

Sample	Metakaolin/g	Na_2SiO_3 Solution/g	NaOH Solution/g	$\text{SiO}_2/\text{Na}_2\text{O}$ Ratio	Water/Solid Ratio
M0.8	1000	722	577	0.8	
M1.0	1000	850	467	1.0	0.8
M1.2	1000	978	357	1.2	
M1.5	1000	1129	226	1.5	

2.2. Test Methods

Final setting time: Modified Vicat test was used to measure the setting time of the geopolymer coating. Under the laboratory conditions of 20 ± 2 °C and $65 \pm 10\%$, the freshly mixed coating material was poured into a glassy mold with a thickness of 2 mm and size of 13 cm \times 13 cm. After the leveling operation, the test method for final hardening time of traditional cement was used to evaluate the hardening time of geopolymer coating with a thickness of 2 mm. The test was carried out as shown in Figure 2a.

Penetration resistance: To study the hardening process of the geopolymer coating, penetration resistance was measured at different times. The freshly mixed geopolymer paste with a volume of 500 mL and thickness of 100 mm, was cast into a plastic container for the penetration resistance. During a time limit of 10 s, a needle with an area of 30 mm² was slowly inserted into 25 mm depth of geopolymer material that measured static pressure force. In general, the test was repeated every 15 min. The test frequency increased as the penetration resistance significantly increased. When the penetration resistance reached 0.7 MPa, the test can be done. The test was carried out as shown in Figure 2b.

The penetration resistance was calculated as follows:

$$f_p = N_p / A_p \quad (1)$$

In which,

f_p is the penetration resistance, MPa;

N_p is the static pressure force at 25 mm depth of geopolymer;

A_p is the area of test needle, 20 mm².



Figure 2. Test for setting behavior of the geopolymer coating. (a) Setting time; (b) Penetration resistance.

Adhesive strength: Chinese standard “Technical code of epoxy resin mortar”, was used to measure the adhesive strength of the coating material. For the test, all specimens had a shape of number 8 (shown in Figure 3). The average of three specimens was taken for the strength test after 7 and 28 days of curing. All the specimens were kept at a constant temperature of 20 ± 2 °C with a relative humidity of $\geq 95\%$. A universal test machine with a capacity of 100 KN was used to measure the adhesive strength of the coating material and mortar by means of axial tensile test.



Figure 3. Test for adhesive strength of the geopolymer coating. (a) Samples for the test of adhesive strength; (b) Fractured surfaces.

Shrinkage deformation: The drying shrinkage and autogenous shrinkage were measured on the specimens with the dimensions of 25 mm × 25 mm × 280 mm. After demolding at 1-day of age, the specimens of autogenous shrinkage were wrapped with an inner layer of plastic foil and an outer layer of aluminum foil. All the shrinkage specimens were exposed in a room at a temperature of 20 ± 2 °C and a relative humidity of 65%. The length of the specimens was monitored using a universal length meter with a measuring accuracy of 0.002 mm. The average length change of at least two specimens was calculated for each mixture.

Chloride resistance: The Nord Test method NT Build 492 [14], was used to measure chloride penetration of concrete coated with a thickness of 2 mm geopolymer coating. The concrete sample was made by 52.5 strength grade Ordinary Portland Cement, and its ratio of water to cement was 0.5. According to the NT Build 492, the chloride migration test was conducted on 50-mm-thick concrete slices after 35 days of curing. When the concrete was cured at the standard condition of 20 ± 2 °C and a relative humidity of 90% until 28 days, the geopolymer coating with various ratios of SiO₂/Na₂O was blade-coated on the concrete surface exposed to a chloride salt solution. The coated concrete was kept in curing at the condition of 20 ± 2 °C and $\geq 95\%$ relative humanity. At the end of the test, silver

nitrate (AgNO_3) was applied to determine chloride penetration. The chloride migration coefficient was then calculated as suggested in [14].

Water uptake test: The test samples were the same as described in the test of chloride resistance. After 28 days of curing at the standard condition, concrete samples were firstly placed in a drying room at 20 ± 2 °C and a relative humidity of 65% for 3 days, and then stored in the oven for drying at the temperature of 50 ± 2 °C for 3 days. Twenty four hours after removing the samples from the oven in the drying room, the geopolymer coating was blade-coated on the concrete surface but the lateral surface was sealed with epoxy coating (Figure 4a), and cured at the standard condition for 7 days. Thereafter, the water uptake test was conducted on the coated concrete samples (Figure 4b). The water absorption rate was defined as the ratio of mass increase to the initial mass of the coated concrete at a different time interval.

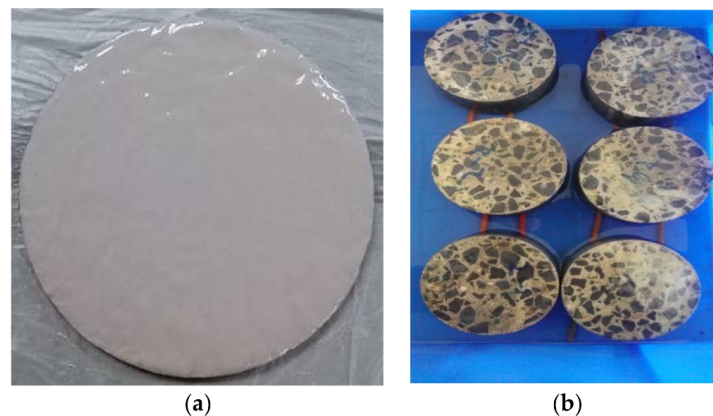


Figure 4. Test for water uptake of the concrete sample coated with the geopolymer coating. (a) Concrete samples coated with the geopolymer coating; (b) Water uptake test for the coated concrete samples.

FTIR analysis: Vibrational bands of the specimens were determined by Fourier Transform Infrared Spectroscopy (FTIR) AVATAR 370 from Thermo Fisher Scientific Inc., Waltham, MA, USA. The KBr pellet technique, about 1 mg powdered sample mixed with 150 mg KBr, was used for the FTIR test. Software OMNIC 8 was used to calculate integration area and peak height of absorption peak.

Pore distribution analysis: The Poremaste GT-60 MIP (Quantachrome, Boynton Beach, FL, USA) was used. The surface tension of mercury was set as 0.48 N/m while the contact angle was 140° . All specimens were firstly crushed into pieces of about $3 \text{ mm} \times 3 \text{ mm} \times 3 \text{ mm}$ at a curing age of 28-day, and stored in absolute alcohol for at least 24 h, then dried at 60 °C for 24 h.

Microstructural morphology: Scanning electron microscopy (SEM, Quanta 250 from FEI) was used to investigate the microstructure of the geopolymer coating. Energy Dispersive Spectrometry (EDS) was used to characterize elemental compositions of micro-zone.

Reaction heat: The heat evolution of each mixed system (10 g paste of metakaolin activated by various usages of alkali solution) was measured using a TAM Air Isothermal calorimeter (Thermometric AB, Järfälla Municipality, Sweden) at 20 °C and ambient pressure.

3. Results

3.1. Setting Time

To study the influence of $\text{SiO}_2/\text{Na}_2\text{O}$ ratio on setting and hardening behaviors of geopolymer coating prepared by alkali-activated metakaolin, Figures 5 and 6 were separately used to characterize the final setting time and penetration resistance of the geopolymer coating. Based on the results described in Figure 5, the final setting time of geopolymer coating with a thickness of 2 mm increased from 260 min to 402 min when the ratio of $\text{SiO}_2/\text{Na}_2\text{O}$ increased from 0.8 to 1.5. Figure 6 shows that the

penetration resistance was stable and then increased steeply. With the increased ratio of $\text{SiO}_2/\text{Na}_2\text{O}$, the penetration resistance of geopolymer coating showed a significantly delayed inflection point. Using the penetration resistance of 0.5 MPa as the threshold value according to the China standard JG/T 70-2009 [15], the setting time increased dramatically which is consistent with the results of final setting time of geopolymer coating with a thickness of 2 mm. The relationship between the final setting time and penetration resistance is depicted in Figure 7. It was observed that the setting time determined by the penetration resistance was a power function of the measured setting time, which was evidenced by the high value of the correlation coefficient.

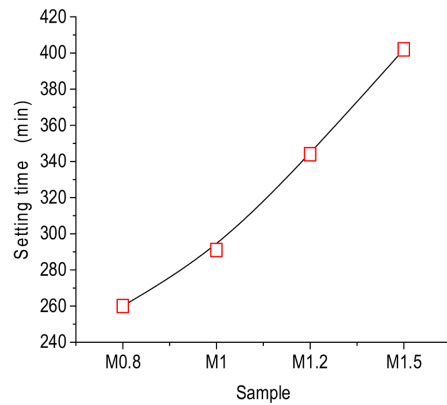


Figure 5. Effect of $\text{SiO}_2/\text{Na}_2\text{O}$ ratio on final setting time of the geopolymer coating.

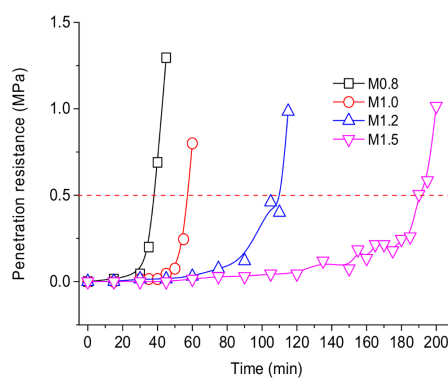


Figure 6. Effect of $\text{SiO}_2/\text{Na}_2\text{O}$ ratio on penetration resistance of the geopolymer coating.

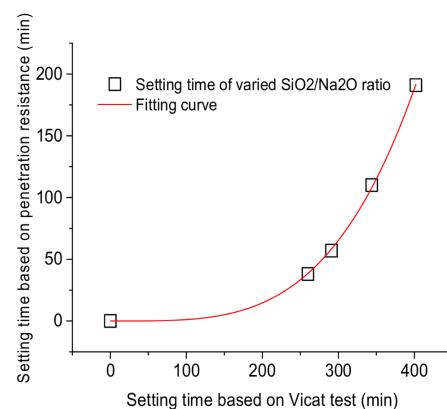


Figure 7. Relationship between the measured results of setting time.

Setting time of the geopolymer coating and bulk increased with the ratio of $\text{SiO}_2/\text{Na}_2\text{O}$. This could be due to the high content of free silicate ions in the alkali solution with a high ratio of $\text{SiO}_2/\text{Na}_2\text{O}$. The high content of free silicate ions led to the formation of geopolymer products on the surface of metakaolin particles in a short duration which inhibited a further polymerization of metakaolin. Therefore, the setting time was delayed. In addition, the setting time determined by the penetration resistance test was lower than that determined by the modified Vicat test. Heat was accumulated from the penetration resistance test since specimens with a volume of 500 mL and a thickness of 100 mm were used. The setting time determined by two different methods displayed a good correlation, which indicated that the ratio of $\text{SiO}_2/\text{Na}_2\text{O}$ can be an important factor affecting setting time of the metakaolin-based geopolymer. It is worth noticing that the final setting time of inorganic polymer coating with a thickness of 2 mm is practical to characterize the hardening behavior of the geopolymer coating.

3.2. Adhesive Strength

The results of adhesive strength are shown in Figures 8–10. From the Figure 8, it is observed that the increased ratio resulted in almost no changes for the adhesive strength at 3 days until a significant decrease as the ratio reached 1.5. Consistent with the 3-day results, the 7-day adhesive strength also decreased dramatically as the ratio of $\text{SiO}_2/\text{Na}_2\text{O}$ increased to 1.5 (Figure 9). In addition, the strength increased with increasing curing time from 3 days to 7 days. Compared with 3 days and 7 days, the geopolymer coating prepared with the ratio of 1.2 exhibited a higher adhesive strength than other ratios at 28 days as shown in Figure 10. In addition, the strength also displayed a higher value for the $\text{SiO}_2/\text{Na}_2\text{O}$ ratio of 1.2 than other ratios. However, the adhesive strength of geopolymer coating with the ratio of 1.5 showed a slightly lower value than that with the ratio of 0.8 and 1.0.

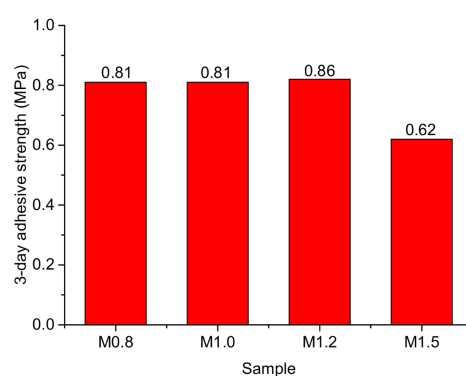


Figure 8. Adhesive strength at the age of 3 days.

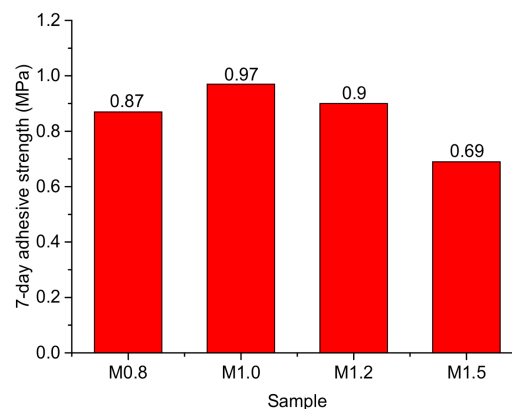


Figure 9. Adhesive strength at the age of 7 days.

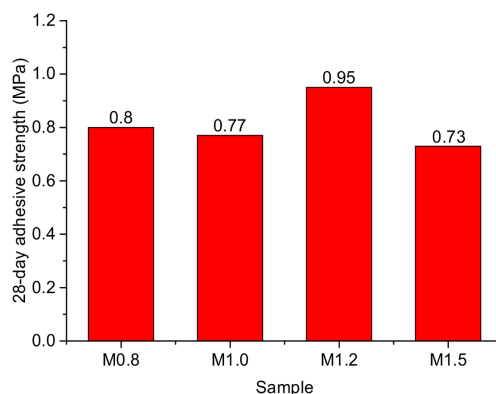


Figure 10. Adhesive strength at the age of 28 days.

3.3. Shrinkage Deformation

Influence of $\text{SiO}_2/\text{Na}_2\text{O}$ ratio on autogenous shrinkage of metakaolin-based geopolymer is shown in Figure 11. The 120 days results revealed that the autogenous shrinkage for the ratio of 1.5 displayed a lower measured result than that of the samples with a ratio of 0.8 and 1.0. From the stage of 1 day to 60 days, the shrinkage for a ratio of 0.8 was close to that for 1.0. However, as the curing age increased from 60 days to 120 days, the autogenous shrinkage increased with an increasing ratio from 0.8 to 1.0. The results indicated that the ratio of 1.0 contributed to geopolymerization of alkali-activated metakaolin after a curing age of 120 days when compared with the ratio of 0.8 and 1.5, which was consistent with the results of adhesive strength described in the previous section. Theoretically, a high ratio of $\text{SiO}_2/\text{Na}_2\text{O}$ increased content of free silicate ions and accelerated geopolymerization of aluminosilicate particles. In that way, the accelerated reaction hindered further reaction between aluminosilicate phases and alkali metal ions. Hence, an increased ratio of $\text{SiO}_2/\text{Na}_2\text{O}$ decreased the autogenous shrinkage.

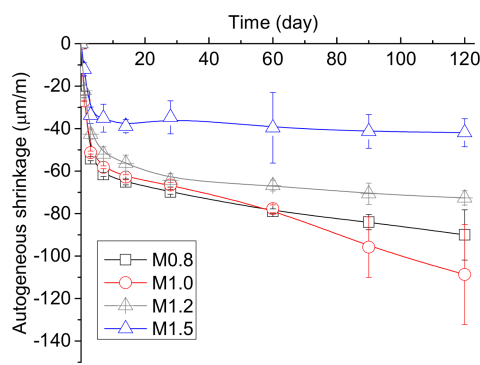


Figure 11. Autogenous shrinkage of the geopolymer coating.

The results of drying shrinkage of the geopolymer prepared with a different ratio of $\text{SiO}_2/\text{Na}_2\text{O}$ are shown in Figure 12. When the ratio of $\text{SiO}_2/\text{Na}_2\text{O}$ increased from 0.8 to 1.5, the drying shrinkage of metakaolin-based geopolymer decreased and then increased at the age of 120 days. The optimal ratio was 1.0 for the metakaolin-based geopolymer which exhibited a lower value of drying shrinkage than the other geopolymer samples.

The drying shrinkage indicated that the optimal ratio of $\text{SiO}_2/\text{Na}_2\text{O}$ can contribute to polycondensation of metakaolin-based geopolymerization. However, high ratios of $\text{SiO}_2/\text{Na}_2\text{O}$ provided excessive amounts of free silicate ions which may hinder a further reaction between the alkali solution and metakaolin. As a result, the microstructure of metakaolin-based geopolymer might be harmed. In addition, the sample with a ratio of 1.5 displayed a higher value of drying shrinkage than

the sample with a ratio of 0.8 and 1.0. This is in good agreement with the results of adhesive strength. Ma et al. [16] found that the results of drying shrinkage of fly ash-based geopolymer decreased when increasing the ratio of $\text{SiO}_2/\text{Na}_2\text{O}$ from 0.7 to 1.0.

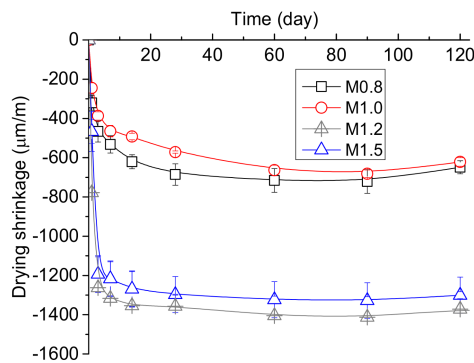


Figure 12. Drying shrinkage of the geopolymer coating.

3.4. Permeability

The influence of geopolymer coating with a thickness of 2 mm on the chloride migration coefficient is shown in Figure 13. The results indicated that the geopolymer coating slightly decreased the chloride migration coefficient of concrete after 7 days of coating. Moreover, it is observed that the concrete samples with the ratio of 1.0 had a lower value of chloride migration coefficient than other samples, which is consistent with the results of adhesive strength and shrinkage deformation. Based on these results, 2 mm thickness of geopolymer coating with the ratio of 1.0 could reduce (by 20 percent) of the chloride migration coefficient as compared with reference concrete. Therefore, we were limited to using geopolymer coating, prepared by alkali-activated metakaolin with a different ratio of $\text{SiO}_2/\text{Na}_2\text{O}$ to improve chloride resistance to concrete.

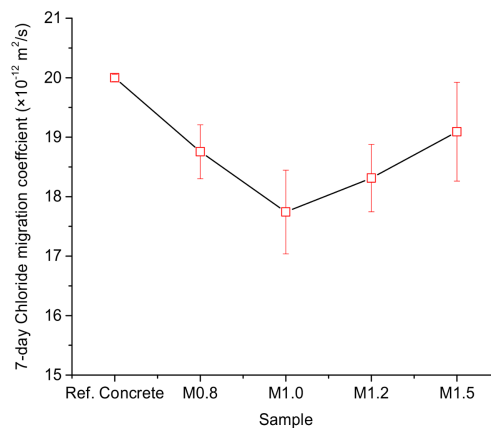


Figure 13. Chloride resistance of concrete sample sealed with the geopolymer coating.

Unlike the results of the chloride penetration mentioned above, influence of the geopolymer coating on decreased 24-h water absorption of concrete samples is significant according to the results in Figure 14. When compared to reference concrete, using the geopolymer coating can reduce water absorption by about 40 to 70 percent. The geopolymer coating prepared by the $\text{SiO}_2/\text{Na}_2\text{O}$ ratio of 1.0 also displayed a better resistance to water uptake than other coatings when immersed in a water tank.

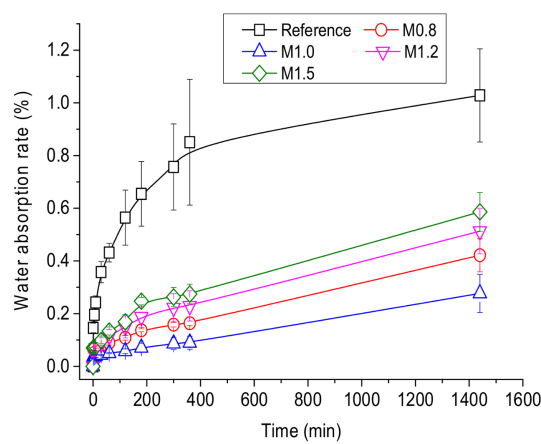


Figure 14. Water uptake of concrete sample sealed with the geopolymer coating.

3.5. Exothermal Rate

Figure 15 indicates that exothermal rate of alkali-activated metakaolin in unit weight decreased greatly when increasing the ratio of $\text{SiO}_2/\text{Na}_2\text{O}$ from 0.8 to 1.5. It is worth of noting that the exothermal rate was decreased by about 50 percent. Besides, some results were summarized as follows: (1) the exothermal peak appeared at the early age, normally in 25 min; (2) the exothermal rate of alkali-activated metakaolin decreased significantly as the ratio of $\text{SiO}_2/\text{Na}_2\text{O}$ was higher than 1.0; (3) the exothermal rate of alkali-activated metakaolin firstly increased dramatically and then decreased until it almost reached zero; (4) Compared to the Portland cement (strength grade of 52.5 MPa) sample with a water to cement ratio of 0.3, the geopolymer sample with an $\text{SiO}_2/\text{Na}_2\text{O}$ ratio of 1.2 and 1.5 exhibited the similar exothermal rate to the Portland cement (see in Figure 15a). However, the Portland cement sample was observed to have a significant exothermal rate at late age than that of the 300 min sample, as shown in Figure 15b. The results of cumulative heat are shown in Figure 16. It is observed that the cumulative heat firstly increased dramatically and then decreased when increasing the ratio from 0.8 to 1.5, which is consistent with the results of the exothermal rate.

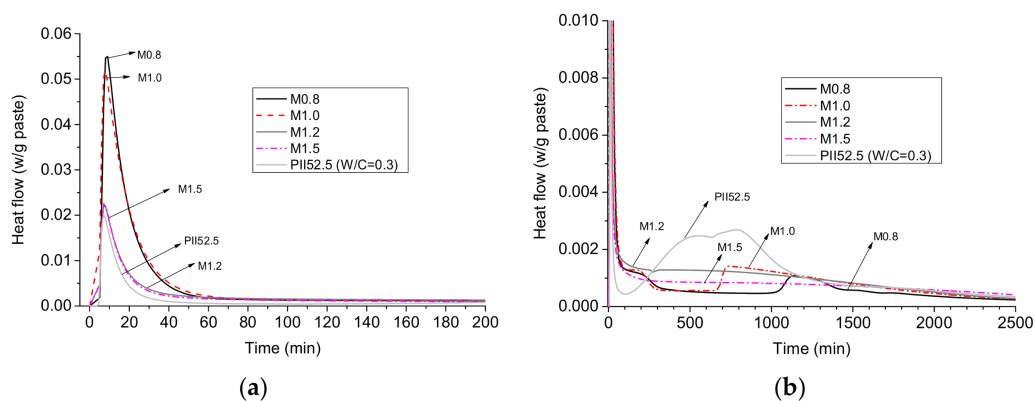


Figure 15. Effect of SiO_2 to Na_2O ratio on exothermal rate of the geopolymer coating. (a) Exothermal rate at early age; (b) Exothermal rate at late age.

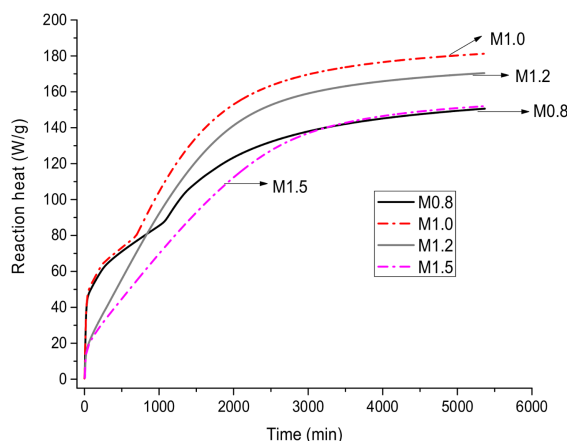


Figure 16. Cumulative heat of the geopolymer coating.

3.6. Pore Structure

Based on the results of pore size distribution in Figure 17, the peak value decreased slightly from 22.24 nm to 20.79 nm as the $\text{SiO}_2/\text{Na}_2\text{O}$ ratio increased from 0.8 to 1.0. However, the peak value increased by 25.80 nm for samples prepared by an $\text{SiO}_2/\text{Na}_2\text{O}$ ratio of 1.5. Besides, the curve of pore size distribution moved forward to the side of small pore sizes with increasing $\text{SiO}_2/\text{Na}_2\text{O}$ ratio from 0.8 to 1.0. On the contrary, increasing the $\text{SiO}_2/\text{Na}_2\text{O}$ ratio to 1.5 resulted in a movement to the side of large pore sizes.

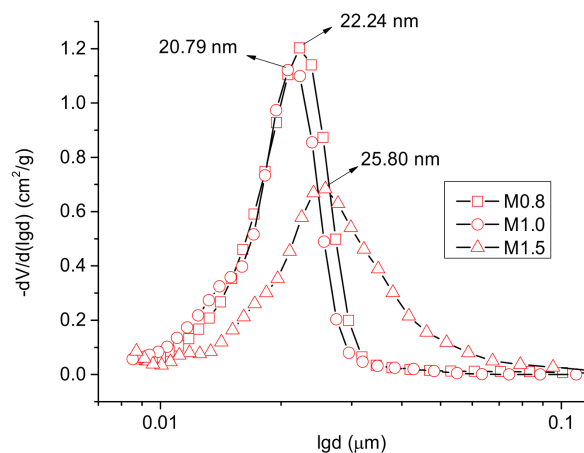


Figure 17. Pore size distribution of the geopolymer coating.

To demonstrate the effect of $\text{SiO}_2/\text{Na}_2\text{O}$ ratio on pore size distribution of the geopolymer, volume percentage and porosity of different pore sizes are shown in Table 3. Compared with the samples prepared by an $\text{SiO}_2/\text{Na}_2\text{O}$ ratio of 0.8 and 1.5, the sample with an $\text{SiO}_2/\text{Na}_2\text{O}$ ratio of 1.0 reduced pore size and porosity and particularly increased volume percentage of pores with a size lower than 20 nm. When the $\text{SiO}_2/\text{Na}_2\text{O}$ ratio increased from 1.0 to 1.5, pores with a size of above 50 nm gained an increase of volume percentage, meanwhile there was a decreased volume percentage of pores with a size below 30 nm. The results of pore size can explain a reduction of adhesive strength of geopolymer as the $\text{SiO}_2/\text{Na}_2\text{O}$ ratio increased from 1.0 to 1.5; even similar porosity was found for samples with an $\text{SiO}_2/\text{Na}_2\text{O}$ ratio of 1.0 and 1.5. Therefore, optimal $\text{SiO}_2/\text{Na}_2\text{O}$ ratio was 1.0 for alkali-activated metakaolin in the present research. Gao et al. [17] also found similar results. The results revealed that the proportion of the macropores (25–5000 nm) decreased when the $\text{SiO}_2/\text{Na}_2\text{O}$ ratio of metakaolin-based geopolymers increased from 1.00 to 1.50. In addition, the macropore volume

increased so that the mesopore (1–25 nm) volume declined when the $\text{SiO}_2/\text{Na}_2\text{O}$ ratio continued to grow.

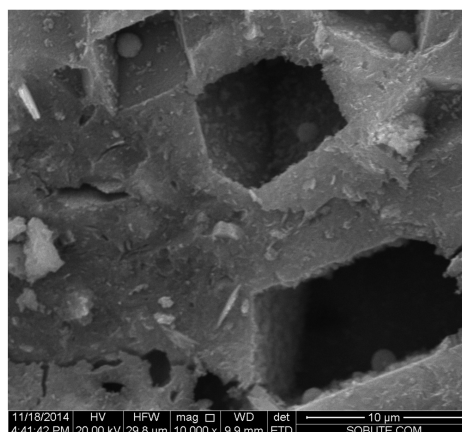
Table 3. Influence of $\text{SiO}_2/\text{Na}_2\text{O}$ ratio on pore size distribution of geopolymer coating.

Sample No.	Pore Size Distribution by Volume Ratio (%)					Porosity (%)
	<10 nm	<20 nm	<30 nm	<50 nm	>50 nm	
M0.8-28 days	1.27	33.91	90.59	93.28	6.72	40.03
M1.0-28 days	2.09	47.61	94.77	97.43	2.57	31.09
M1.5-28 days	1.70	20.96	60.94	88.15	11.85	30.97

Compared with the $\text{SiO}_2/\text{Na}_2\text{O}$ ratio of 0.8, the modulus of 1.0 decreased volume percentage of 50 nm of pore size for geopolymer sample. Besides, porosity of the geopolymer sample was reduced by 9% in volume. The result of pore size and porosity could restraint drying shrinkage of the geopolymer due to impeding water evaporation. By contrast, an $\text{SiO}_2/\text{Na}_2\text{O}$ ratio of 1.5 caused an obstacle for polymerization of Si-Al phase and microstructure development in that free silicate ions condensed on the surface of metakaolin particles to form polymerization products and resulting in dense reaction layers. Therefore, a high $\text{SiO}_2/\text{Na}_2\text{O}$ ratio resulted in a significant increase of volume percentage of pores with a size above 50 nm, which could be the reason for a high value of drying shrinkage of geopolymer.

3.7. SEM

Figure 18 demonstrates the microstructure patterns of alkali-activated metakaolin prepared by different $\text{SiO}_2/\text{Na}_2\text{O}$ ratios. Based on the observed results from Figure 18a–c, it was found that microstructure of geopolymer changed from a porous structure to a dense structure and became a poor structure as the ratio increased. Gao et al. [17] reported that metakaolin-based geopolymer with an $\text{SiO}_2/\text{Na}_2\text{O}$ ratio of 1.50 exhibited the most compact microstructure at the condition of heat curing. Liew et al. [18] observed that a geopolymer sample with an $\text{Na}_2\text{SiO}_3/\text{NaOH}$ ratio of 0.20 has more geopolymeric gel with more intervening materials than the samples with the ratio of 0.12 and 0.28.



(a)

Figure 18. Cont.

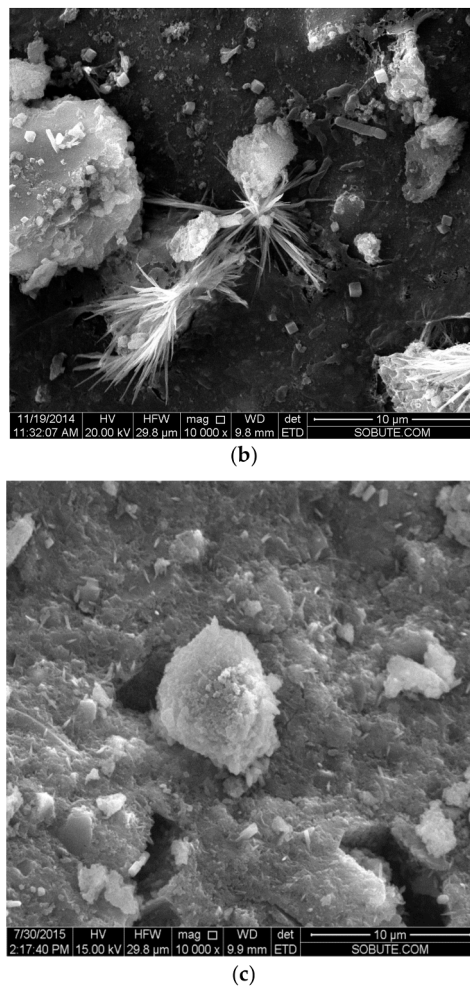


Figure 18. SEM pattern of the geopolymer coating at the age of 28 days. (a) M0.8; (b) M1.0; (c) M1.5.

Compared with an $\text{SiO}_2/\text{Na}_2\text{O}$ ratio of 0.8 and 1.5, needle-shaped products prepared was observed for an $\text{SiO}_2/\text{Na}_2\text{O}$ ratio of 1.0 (see Figure 18b). The needle product could be a crystallite phase of zeolite according to the model reported by Provis et al. [19,20]. As for the geopolymerization, gel phase undergoes a continuous rearrangement and becomes more crosslinked with a release of unbound water. Besides, some zeolitic crystallites are also formed in the geopolymerization. Figure 19 displayed the pattern of Energy Dispersive X-ray Analysis for the needle product. It was observed that the main elements are composed of Silica, Aluminum, Oxygen and Sodium, which supports the suggestion that the needle product could be zeolite crystallite.

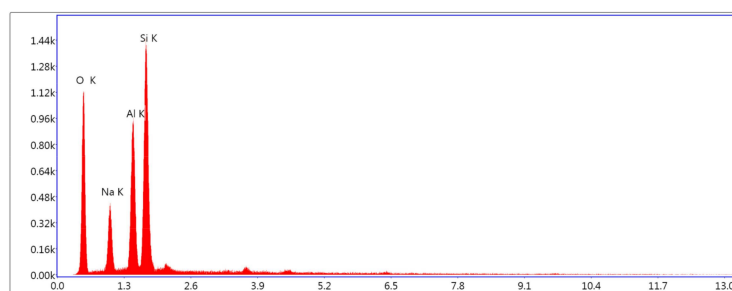


Figure 19. Element analysis of needle product from M1.0.

3.8. FTIR Analysis

Figure 20 presents the FTIR spectra of the metakaolin-based geopolymer with various $\text{SiO}_2/\text{Na}_2\text{O}$ ratios at 3 days. The alkali activation of metakaolin formed a broad band of OH^- stretching vibration located at around 3450 cm^{-1} in the geopolymer product. Besides, the band of 1649 cm^{-1} is associated with OH^- or H_2O bending vibration, which is thought of as weak H_2O bond adsorbed at the surface or caught in cavities of the geopolymer structure. With the increase of $\text{SiO}_2/\text{Na}_2\text{O}$ ratio, there is an increased intensity of the bands at 3450 cm^{-1} and 1649 cm^{-1} . This result indicated that more water molecules or OH^- were included in the structure of geopolymer with a high $\text{SiO}_2/\text{Na}_2\text{O}$ ratio, which might be explained by the inhibition of water evaporation in a dense microstructure.

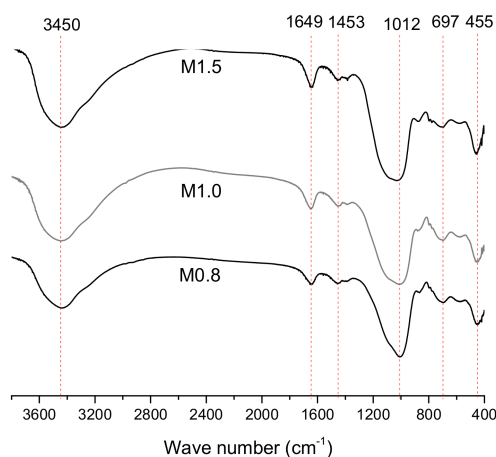


Figure 20. FTIR spectra of 3-day geopolymer coating.

The apparent bond at approximately 1453 cm^{-1} is attributed to O-C-O stretching vibration due to a reaction between alkali-metal hydroxide and the atmospheric CO_2 [21]. The region at $950\text{--}1200\text{ cm}^{-1}$ is assigned to asymmetric stretching vibration of Si-O-Si or Si-O-Al, which is often used to determine the degree of polymerization [22]. In addition, the band of $1012\text{--}1016\text{ cm}^{-1}$ displayed a shift to a high frequency, which indicates that the polymerization degree strengthened [21,23]. This result implied that the $\text{SiO}_2/\text{Na}_2\text{O}$ ratio increased from 0.8 to 1.5 and contributed to geopolymerization. However, results from Lee et al. [24] suggested that geopolymer prepared by an $\text{SiO}_2/\text{Na}_2\text{O}$ ratio of 1.0 was likely to produce more heterogeneous geopolymer because of a greater silicate structural reorganization involving formation of crystallization which has been proven by SEM patterns.

In Figure 21, the absorption peaks at 697 and 455 cm^{-1} were, respectively, attributed to Al-O-Si and Si-O-Si of bending vibration in Kaolinite. Compared with M0.8 and M1.0, M1.5 has a higher intensity of absorption peak, which meant that less metakaolin is dissolved in a system of alkali-activated metakaolin prepared by an $\text{SiO}_2/\text{Na}_2\text{O}$ ratio of 1.5. This result is consistent with a reduction of adhesive strength of geopolymer as $\text{SiO}_2/\text{Na}_2\text{O}$ ratio increased from 1.0 to 1.5. Figure 21 manifests the FTIR spectra of the metakaolin-based geopolymer with various $\text{SiO}_2/\text{Na}_2\text{O}$ ratios at 28 days of age. At 28 days, the FTIR spectra showed similarity to the characteristic absorption band at 3 days. However, there is still some dissimilarity: (a) With the increase in curing time, the band at 1453 cm^{-1} was diminished, which indicated that carbonation of alkali-metal hydroxide was not obvious for the sample at 28 days. (b) Compared with 3 days, the band at 3444 cm^{-1} shifted to a low wavenumber, but the bands at 1653 , 1016 and 702 cm^{-1} underwent a slight shift toward higher wavenumbers. On one hand, the latter result suggested that increased curing age contributed to a polymerization degree of alkali-activated metakaolin. On the other hand, the opposite change of absorption band, at approximately 3440 to 3450 cm^{-1} , indicated that water molecules or OH^- were transformed from stretching to bending vibration. The reason for the transformation could be that unbalanced charge

from the Al phase replaced Si phase which affected vibration behavior of water molecules or OH^- with the increase of polymerization degree at 28 days.

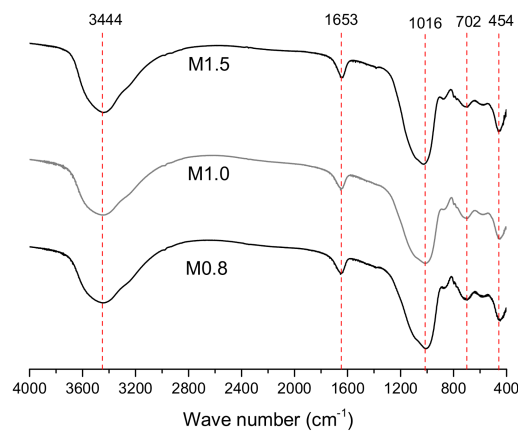


Figure 21. FTIR spectra of 28-day geopolymer coating.

4. Discussion

Based on the theory of geopolymerization proposed by Duxson et al. [10], dissolution of aluminate and silicate minerals and equilibrium of ionic species were the initial steps of microstructure formation of alkali-activated materials. In the present research, increasing the usage of liquid sodium silicate and decreasing the usage of NaOH solution, led to an increased content of free and chemically active silicate ions but a decrease of content of sodium and hydroxyl ions. Zhang et al. [25] thought that the increased contents of Si and Al in the aqueous phase enhanced the formation of the oligomeric precursors due to the increased dissolution rates. Gao et al. [17] thought that the increased ratio of $\text{SiO}_2/\text{Na}_2\text{O}$ contributed to aluminosilicate dissolution and the 3D polymeric framework which is respective to the high mechanical properties.

At the early age of geopolymerization, the increased content of silicate ions contributed to the hydrolysis reaction and gelation of silicate monomers and oligomers, which increased the viscosity of paste and inhibited the geopolymerization due to lump and poor dispense of metakaolin particles at the step of fresh paste. The results turned into a delay of setting and hardening behavior of metakaolin-based geopolymer. Heah et al. [26] reported that the high content of the sodium-silicate solution caused the geopolymer paste to become sticky because of the viscous nature of the sodium-silicate solution. In addition, results from Gao et al. [17] also proved that the initial and final setting times increased significantly when the $\text{SiO}_2/\text{Na}_2\text{O}$ ratio increased by addition of nano- SiO_2 . Consistent with the reported results mentioned above, the present research found that the setting time of geopolymer coating made by metakaolin-based geopolymer increased when the $\text{SiO}_2/\text{Na}_2\text{O}$ ratio increased from 0.8 to 1.5. The decreased value of penetration resistance with increasing time also supported the result. In addition, the exothermal rate of alkali-activated metakaolin decreased significantly as the ratio of $\text{SiO}_2/\text{Na}_2\text{O}$ was higher than 1.0 at the early age of 60 min.

As for the strength and permeability, it can be observed that a threshold value for the content of silicate ions is represented by $\text{SiO}_2/\text{Na}_2\text{O}$ ratio. When the ratio surpasses the threshold value, microstructural defects developed in the geopolymer which decreases the strength and increases the permeability and poor flowability resulted from a viscous paste. As a matter of fact, the present research found that the adhesive strength of the geopolymer coating material firstly increased and then decreased with the $\text{SiO}_2/\text{Na}_2\text{O}$ ratio. The geopolymer coating prepared by the $\text{SiO}_2/\text{Na}_2\text{O}$ ratio of 1.0 displayed a better resistance to water uptake and chloride transport than other coatings with a different $\text{SiO}_2/\text{Na}_2\text{O}$ ratio. In addition, FTIR testing results also implied that geopolymer prepared by $\text{SiO}_2/\text{Na}_2\text{O}$ ratio of 1.0 was likely to produce more heterogeneous geopolymer because of a greater silicate structural reorganization involving formation of crystallization which has been

proven by SEM results in the present study. Gao et al. [17] found a threshold value of $\text{SiO}_2/\text{Na}_2\text{O}$ ratio for metakaolin-based geopolymer is 1.5. When surpassing the value, the strength of geopolymer decreased but the macropore volume increased so that the mesopore volume declined. Consistent with the result, the present research also observed that the volume percentage of pores with a size of above 50 nm increased by about 9.3 percent when the geopolymer coating increased the ratio of $\text{SiO}_2/\text{Na}_2\text{O}$ from 1.0 to 1.5, which could be the reason for the decreased strength and permeability, and a high value of drying shrinkage of geopolymer. In addition, low content of soluble silica resulted in a high aluminum content of gel (Al-rich gel) which has been proved to be lower mechanical strength than the Si-rich gel [27,28]. Based on the results reported by some studies [29–32], it is widely accepted that there is an optimum $\text{SiO}_2/\text{Na}_2\text{O}$ ratio for alkali-activated materials, including metakaolin, fly ash and aluminosilicate waste.

As for the reduced strength of geopolymer at a late age, it was observed that high ratio of $\text{SiO}_2/\text{Na}_2\text{O}$ was helpful to decrease the amplitude of strength and avoiding the attack of hydrolysis ions on microstructure of geopolymer at a late age. Consistent with this result, Pelisser et al. [32] also showed decreased strength with an increasing age. Besides, according to the results of present research, a high value of drying shrinkage respective to a high $\text{SiO}_2/\text{Na}_2\text{O}$ ratio also can cause micro defects into the hardened geopolymer so as to decrease the strength of geopolymer coating material at the age of 60 days. However, the mechanism for strength decreasing of alkali-activated materials is worth further investigation in future.

5. Conclusions

Some conclusions can be drawn from this study as follows:

- (1) The setting time of metakaolin-based geopolymer coating increased when the $\text{SiO}_2/\text{Na}_2\text{O}$ ratio increased from 0.8 to 1.5, as revealed from the penetration resistance test. The significant decrease of exothermal rate of alkali-activated metakaolin at the early age of 60 min also proves the role of setting delay when the $\text{SiO}_2/\text{Na}_2\text{O}$ ratio increases.
- (2) The optimal $\text{SiO}_2/\text{Na}_2\text{O}$ ratio can assure a good result for the adhesive strength and permeability. The experimental results indicated that the geopolymer coating prepared by the $\text{SiO}_2/\text{Na}_2\text{O}$ ratio of 1.0 displayed a novel resistance to water uptake and chloride transport. When the ratio was higher than the optimal value, microstructural defects developed in the geopolymer decreased the strength and increased the permeability in that poor flowability resulted from viscous paste.
- (3) The autogenous shrinkage at 120 days suggested that a ratio of 1.0 displayed a higher value than the ratios of 0.8 and 1.5. Corresponding to the autogenous shrinkage, the geopolymer sample with an optimal ratio of 1.0 exhibited a lower value of drying shrinkage than the other samples.
- (4) The geopolymer coating with the ratio of 1.0, exhibited a refined pore size distribution and decreased porosity. Results of Fourier Transform Infrared Spectroscopy (FTIR) implied that increase of the ratio contributed to geopolymerization. Besides, geopolymer prepared by the ratio of 1.0 was likely to produce more heterogeneous geopolymer due to a greater silicate structural reorganization.

Acknowledgments: Authors appreciate the financial supports from the National Key R & D Program of China under the contract No. 2017YFB0309904, the National Basic Research Program of China (973 Program) under the contract No. 2015CB655105, the Science and Technology Planning Project of Jiangsu Province under the contract No. BE2017158, and the Science and technology project of China Electric Power Engineering Consultant Group Co., Ltd. under the contract No. DG1-T02-2017, and the Shenzhen Key Laboratory of Civil Engineering Durability under the contract No. GDDCE1613.

Author Contributions: Song Mu and Jianzhong Liu designed the experiments; Liang Shi and Qian Jiang contributed materials and performed the experiments; Yaocheng Wang and Jianzhong Liu analyzed the data; Song Mu and Jiaping Liu wrote the paper.

Conflicts of Interest: The authors declare no conflict of interest.

References

1. Brito, M.; Case, E.; Kriven, W.M.; Salem, J.; Zhu, D. Corrosion Protection Assessment of Concrete Reinforcing Bars with a Geopolymer Coating. In *Developments in Porous, Biological and Geopolymer Ceramics: Ceramic Engineering and Science Proceedings*; Wiley: Hoboken, NJ, USA, 2009.
2. Temuujin, J.; Minjigmaa, A.; Rickard, W.; Lee, M.; Williams, I.; van Riessen, A. Preparation of metakaolin based geopolymer coatings on metal substrates as thermal barriers. *Appl. Clay Sci.* **2009**, *46*, 265–270. [[CrossRef](#)]
3. Zhang, Z.; Yao, X.; Wang, H. Potential application of geopolymers as protection coatings for marine concrete III. Field experiment. *Appl. Clay Sci.* **2010**, *49*, 491–496. [[CrossRef](#)]
4. Temuujin, J.; Minjigmaa, A.; Rickard, W.; Lee, M.; Williams, I.; van Riessen, A. Fly ash based geopolymer thin coatings on metal substrates and its thermal evaluation. *J. Hazard. Mater.* **2010**, *180*, 748–752. [[CrossRef](#)] [[PubMed](#)]
5. Khan, M.I.; Azizli, K.; Sufian, S.; Man, Z. Sodium silicate-free geopolymers as coating materials: Effects of Na/Al and water/solid ratios on adhesion strength. *Ceram. Int.* **2014**, *41*, 2794–2805. [[CrossRef](#)]
6. Vidal, L.; Joussein, E.; Absi, J.; Rossignol, S. Coating of unreactive and reactive surfaces by aluminosilicate binder. *Ceram. Int.* **2016**, *43*, 1819–1829. [[CrossRef](#)]
7. Aguirre-Guerrero, A.M.; Robayo-Salazar, R.A.; Gutiérrez, R.M.D. A novel geopolymer application: Coatings to protect reinforced concrete against corrosion. *Appl. Clay Sci.* **2017**, *135*, 437–446. [[CrossRef](#)]
8. Davidovits, J. Geopolymers. *J. Therm. Anal.* **1991**, *37*, 1633–1656. [[CrossRef](#)]
9. Duxson, P.; Provis, J.L.; Lukey, G.C.; Mallicoat, S.W.; Kriven, W.M.; van Deventer, J.S.J. Understanding the relationship between geopolymer composition, microstructure and mechanical properties. *Colloid Surf. A* **2005**, *269*, 47–58. [[CrossRef](#)]
10. Duxson, P.; Fernández-Jiménez, A.; Provis, J.L.; Lukey, G.C.; Palomo, A.; van Deventer, J.S.J. Geopolymer technology: The current state of the art. *J. Mater. Sci.* **2007**, *42*, 2917–2933. [[CrossRef](#)]
11. Fernández-Jiménez, A.; Palomo, A.; Criado, M. Microstructure development of alkali-activated fly ash cement: A descriptive model. *Cem. Concr. Res.* **2005**, *35*, 1204–1209. [[CrossRef](#)]
12. Park, S.M.; Jang, J.G.; Lee, N.K.; Lee, H.K. Physicochemical properties of binder gel in alkali-activated fly ash/slag exposed to high temperatures. *Cem. Concr. Res.* **2016**, *89*, 72–79. [[CrossRef](#)]
13. Park, S.M.; Jang, J.G.; Chae, S.A.; Lee, H.K. An NMR spectroscopic investigation of aluminosilicate gel in alkali-activated fly ash in a CO₂-rich environment. *Materials* **2016**, *9*, 308. [[CrossRef](#)] [[PubMed](#)]
14. Nord Test. NT Build 492, Chloride Migration Coefficient from Non-Steady State Migration Experiments. UDC 691.32/691.53/691.54, November 1999.
15. Chinese Construction Industry Standard. JGJ/T 70–2009, *Standard for Test Method of Performance on Building Mortar*; China Architecture & Building Press: Beijing, China, 2009. (In Chinese)
16. Ma, Y.; Ye, G. The shrinkage of alkali activated fly ash. *Cem. Concr. Res.* **2015**, *68*, 75–82. [[CrossRef](#)]
17. Gao, K.; Lin, K.L.; Wang, D.Y.; Hwang, C.L.; Shiu, H.S.; Chang, Y.M.; Cheng, T.W. Effects SiO₂/Na₂O molar ratio on mechanical properties and the microstructure of nano-SiO₂, metakaolin-based geopolymers. *Constr. Build. Mater.* **2014**, *53*, 503–510. [[CrossRef](#)]
18. Liew, Y.M.; Kamarudin, H.; Bakri, A.M.M.A.; Bnhussain, M.; Luqman, M.; Khairul Nizar, I.; Ruzaidi, C.M.; Heah, C.Y. Optimization of solids-to-liquid and alkali activator ratios of calcined kaolin geopolymeric powder. *Constr. Build. Mater.* **2012**, *37*, 440–451. [[CrossRef](#)]
19. Provis, J.L. Modeling the Formation of Geopolymers. Ph.D. Thesis, Department of Chemical and Biomolecular Engineering, The University of Melbourne, Melbourne, Australia, 2006.
20. Provis, J.L.; van Deventer, J.S.J. Geopolymerisation kinetics. 2. Reaction kinetic modelling. *Chem. Eng. Sci.* **2007**, *62*, 2318–2329. [[CrossRef](#)]
21. Andini, S.; Cioffi, R.; Colangelo, F.; Grieco, T.; Montagnaro, F.; Santoro, L. Coal fly ash as raw material for the manufacture of geopolymer-based products. *Waste Manag.* **2008**, *28*, 416–423. [[CrossRef](#)] [[PubMed](#)]
22. Chindapasirt, P.; Chai, J.; Chalee, W.; Rattanasak, U. Comparative study on the characteristics of fly ash and bottom ash geopolymers. *Waste Manag.* **2009**, *29*, 539–543. [[CrossRef](#)] [[PubMed](#)]
23. Bernal, S.A.; Provis, J.L.; Rose, V.; De Gutierrez, R.M. Evolution of binder structure in sodium silicate-activated slag-metakaolin blends. *Cem. Concr. Compos.* **2011**, *33*, 46–54. [[CrossRef](#)]

24. Lee, W.K.W.; van Deventer, J.S.J. Structural reorganization of class F fly ash in alkaline silicate solutions. *Colloids Surf. A* **2002**, *211*, 49–66. [[CrossRef](#)]
25. Zhang, Z.H.; Yao, X.; Zhu, H.J. Role of water in the synthesis of calcined kaolin based geopolymer. *Appl. Clay Sci.* **2009**, *43*, 218–223. [[CrossRef](#)]
26. Heah, C.Y.; Kamarudin, H.; Mustafa Al Bakri, A.M.; Brhussain, M.; Luqman, M.; Khairul Nizar, I.; Ruzaidi, C.M.; Liew, Y.M. Study on solids-to-liquid and alkaline activator ratios on kaolinbased geopolymers. *Constr. Build. Mater.* **2012**, *35*, 912–922. [[CrossRef](#)]
27. Criado, M.; Fernández-Jiménez, A.; Palomo, A. Alkali activation of fly ash: Effect of the SiO₂/Na₂O ratio: Part I: FTIR study. *Microporous Mesoporous Mater.* **2007**, *106*, 180–191. [[CrossRef](#)]
28. Fernández-Jiménez, A.; Palomo, A.; Sobrados, I.; Sanz, J. The role played by the reactive alumina content in the alkaline activation of fly ashes. *Microporous Mesoporous Mater.* **2006**, *91*, 111–119. [[CrossRef](#)]
29. Tashima, M.M.; Akasaki, J.L.; Castaldelli, V.N.; Soriano, L.; Monzó, J.; Payá, J.; Borrachero, M.V. New geopolymeric binder based on fluid catalytic cracking catalyst residue (FCC). *Mater. Lett.* **2012**, *80*, 50–52. [[CrossRef](#)]
30. Lampris, C.; Lupo, R.; Cheeseman, C.R. Geopolymerisation of silt generated from construction and demolition waste washing plants. *Waste Manag.* **2009**, *29*, 368–373. [[CrossRef](#)] [[PubMed](#)]
31. Wu, H.C.; Sun, P. New building materials from fly ash-based lightweight inorganic polymer. *Constr. Build. Mater.* **2007**, *21*, 211–217. [[CrossRef](#)]
32. Pelisser, F.; Guerrino, E.L.; Menger, M.; Labrincha, J.A. Micromechanical characterization of metakaolin-based geopolymers. *Constr. Build. Mater.* **2013**, *49*, 547–553. [[CrossRef](#)]



© 2018 by the authors. Licensee MDPI, Basel, Switzerland. This article is an open access article distributed under the terms and conditions of the Creative Commons Attribution (CC BY) license (<http://creativecommons.org/licenses/by/4.0/>).